Activin B receptor ALK7 is a negative regulator of pancreatic β-cell function

Philippe Bertolino*, Rebecka Holmberg†, Eva Reissmann*, Olov Andersson*, Per-Olof Berggren†, and Carlos F. Ibáñez*‡

*Division of Molecular Neurobiology, Department of Neuroscience and †Rolf Luft Research Center for Diabetes and Endocrinology, Karolinska Institutet, S-17177 Stockholm, Sweden

Edited by Robert J. Lefkowitz, Duke University Medical Center, Durham, NC, and approved March 18, 2008 (received for review February 8, 2008)

All major cell types in pancreatic islets express the transforming growth factor (TGF)-β superfamily receptor ALK7, but the physiological function of this receptor has been unknown. Mutant mice lacking ALK7 showed normal pancreas organogenesis but developed an age-dependent syndrome involving progressive hyperinsulinemia, reduced insulin sensitivity, liver steatosis, impaired glucose tolerance, and islet enlargement. Hyperinsulinemia preceded the development of any other defect, indicating that this may be one primary consequence of the lack of ALK7. In agreement with this, mutant islets showed enhanced insulin secretion under sustained glucose stimulation, indicating that ALK7 negatively regulates glucose-stimulated insulin release in β-cells. Glucose increased expression of ALK7 and its ligand activin B in islets, but decreased that of activin A, which does not signal through ALK7. The two activins had opposite effects on Ca^{2+} signaling in islet cells, with activin A increasing, but activin B decreasing, glucose-stimulated Ca^{2+} influx. On its own, activin B had no effect on WT cells, but stimulated Ca^{2+} influx in cells lacking ALK7. In accordance with this, mutant mice lacking activin B showed hyperinsulinemia comparable with that of *Alk7*$^{-/-}$ mice, but double mutants showed no additive effects, suggesting that ALK7 and activin B function in a common pathway to regulate insulin secretion. These findings uncover an unexpected antagonism between activins A and B in the control of Ca^{2+} signaling in β-cells. We propose that ALK7 plays an important role in regulating the functional plasticity of pancreatic islets, negatively affecting β-cell function by mediating the effects of activin B on Ca^{2+} signaling.

calcium | insulin | pancreas | TGF-β | hyperinsulinemia

The signaling networks controlling metabolic processes are highly regulated and integrate the actions of both positively and negatively acting components from many different signaling pathways. Members of the transforming growth factor (TGF)-β superfamily, including TGF-βs, growth and differentiation factors (GDFs), bone morphogenetic proteins (BMPs) and activins, have been implicated in the regulation of several metabolic processes. These ligands signal via distinct complexes of type I and type II receptor serine–threonine kinases, each binding to different classes of TGF-β ligands (1, 2). The main and most widely studied signaling pathway downstream of these receptors involves activation and nuclear translocation of Smad proteins, which in turn regulate gene transcription through multiple interactions with distinct sets of transcription factors in a cell type-specific manner (1, 2). Although less well understood, Smad-independent pathways have also been described in a variety of cell systems and involve the activation of MAP kinases, small GTPases, and Ca^{2+} mobilization (3).

Identification of cell-intrinsic factors controlling the specification and function of pancreatic endocrine cells is of major importance for understanding the regulation of blood-glucose homeostasis. The characterization of signals regulating β-cell development and insulin production and secretion has been the focus of intense work. Although the importance of activin signaling for pancreas development and β-cell differentiation is well established (4, 5), much less is known about the physiological functions of activins and related ligands in adult pancreatic islets *in vivo*. Activins A and -B are expressed in islet cells, suggesting autocrine and/or paracrine roles within islets (6, 7). *In vitro* experiments have indicated an ability of activin A to increase cytoplasmic free Ca^{2+} concentration ($[Ca^{2+}]_i$) and induce insulin secretion in β-cells even at very low levels of ambient glucose (8, 9). In contrast, the biological activities of activin B in islet cells are still unknown. The multiple developmental defects presented by null mutants of type I and type II activin receptors have limited the utility of those animal models for understanding the physiological actions of activins in adult pancreatic islets. A more recent report has indicated that mice lacking the activin inhibitor follistatin-like 3 (FSTL3) develop enlarged pancreatic islets and a moderate increase in insulin serum levels by 9 months of age (10), consistent with a positive role for activins in islet development and function. In addition, conditional adult overexpression of Smad7, a potent cytoplasmic inhibitor of TGF-β and activin signaling, reduced pancreatic insulin content and produced severe hypoinsulinemia (11), indicating an essential role for ongoing TGF-β signaling in the maintenance of β-cell function.

The type I receptor ALK7 can mediate signaling by a selected group of ligands in the TGF-β superfamily, including Nodal (12), GDF-1 (13), GDF-3 (14) and activin B (15), all of which can also signal through the ubiquitous activin type I receptor ALK4. Unlike ALK4, however, ALK7 does not mediate activin A signaling (15, 16). ALK7 is dispensable for mouse embryogenesis (17), which suggests alternative functions for this receptor in postnatal development and tissue homeostasis. ALK7 is expressed in several organs involved in metabolic regulation, including pancreas, adipose tissue, gut, and brain (16, 18–20), but the physiological function of this receptor has been unknown. In this study, we have investigated the roles of ALK7 in metabolic control and the organization and function of the endocrine pancreas.

Results

Age-Dependent Hyperinsulinemia, Reduced Insulin Sensitivity, Impaired Glucose Tolerance, and Liver Steatosis in *Alk7*$^{-/-}$ Mice. After weaning, *Alk7*$^{-/-}$ mice gained weight to a similar extent as WT animals and showed normal fasting levels of glucose and glucagon in serum [supporting information (SI) Fig. S1]. However, the mutants displayed significantly increased insulin serum levels starting at 2 weeks of age (Fig. 1*A*). Insulin responses were normal in 2-week-old mutant mice (Fig. 1*B*), but 2- and 5-month-old mutants showed reduced insulin sensitivity compared with

Author contributions: P.B., P.-O.B., and C.F.I. designed research; P.B., R.H., E.R., and O.A. performed research; P.B., R.H., P.-O.B., and C.F.I. analyzed data; and P.B., P.-O.B., and C.F.I. wrote the paper.

The authors declare no conflict of interest.

This article is a PNAS Direct Submission.

‡To whom correspondence should be addressed. E-mail: carlos.ibanez@ki.se.

This article contains supporting information online at www.pnas.org/cgi/content/full/0801285105/DCSupplemental.

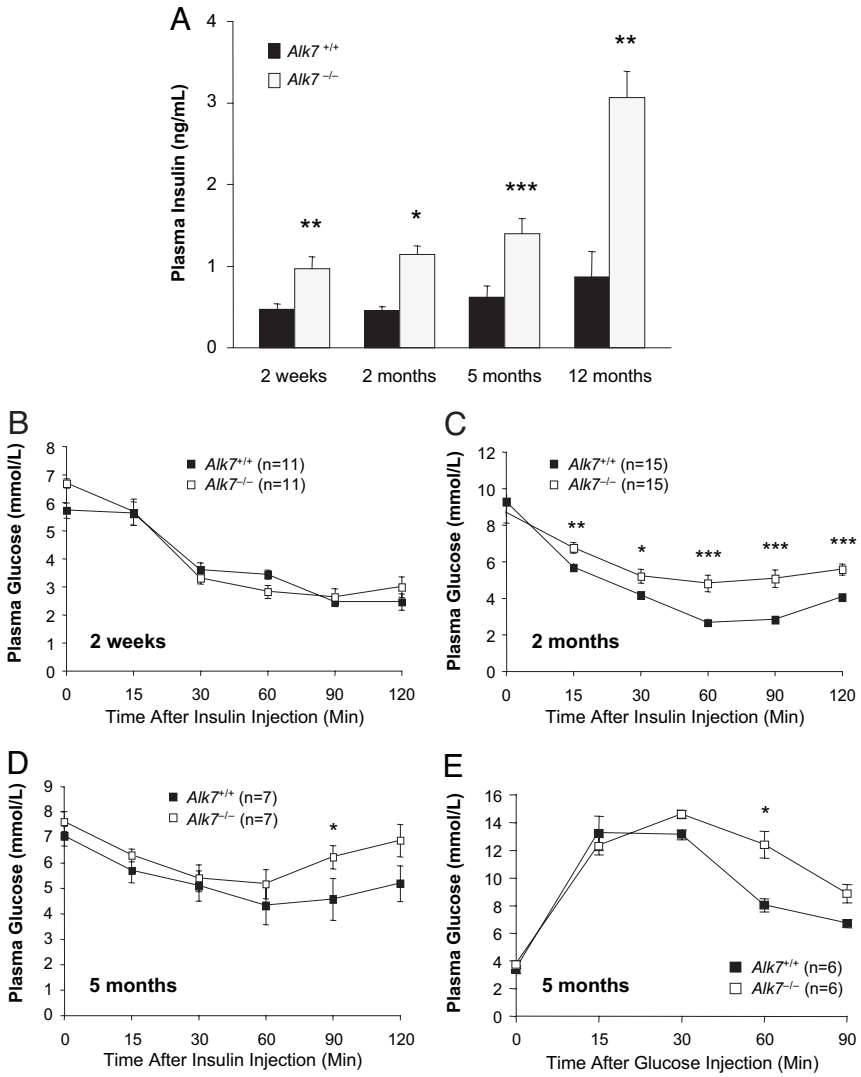

Fig. 1. Hyperinsulinemia and reduced insulin sensitivity and glucose tolerance in *Alk7*$^{-/-}$ mice. (*A*) Insulin serum levels after overnight fasting in WT and *Alk7*$^{-/-}$ mice. Results are expressed as average ± SEM (n = 11–27). *, $P \leq 0.05$; **, $P < 0.01$; ***, $P < 0.001$ vs. WT (Student's t test). (*B–D*) Insulin tolerance test of 2-week-, 2-month-, and 5-month-old *Alk7*$^{-/-}$ mutant and WT mice after 3-h fasting. Results are expressed as average ± SEM. *, $P \leq 0.05$; **, $P < 0.01$; ***, $P < 0.001$ vs. WT (Student's t test). (*E*) Glucose tolerance test of 5-month-old Alk7$^{-/-}$ mutant and WT mice. Results are expressed as average ± SEM (n = 6 animals). *, $P \leq 0.05$ vs. WT (Student's t test).

age-matched WT controls (Fig. 1 *C* and *D*). In addition, impaired glucose tolerance responses were observed in 5-month-old mutant mice (Fig. 1*E*). At 12 months of age, *Alk7*$^{-/-}$ mice developed pronounced liver steatosis (Fig. 2*A*). Liver weight was increased by 20–25% in the mutants from 2 months onwards (Fig. 2*B*), and at 5 months, triglyceride content in livers of *Alk7*$^{-/-}$ mice was almost doubled compared with WT controls (Fig. 2*C*). Histological analysis of liver sections by Oil red-O staining revealed a progressive increase in liver lipid deposition in the mutants starting from 2 months of age (Fig. 2*D*). The livers of 2-week-old mutants were indistinguishable from those of WT (Fig. 2*D*), which is in line with the absence of insulin resistance at this age.

Alk7 Expression in Mouse Endocrine Pancreas. The fact that hyperinsulinemia was the first abnormality found to appear in the mutants directed our attention to the organization and function of the endocrine pancreas. Previous work has indicated that ALK7 may be expressed in insulin-producing β-cells (15), or in both β- and α-cells (21). The *LacZ* reporter gene inserted in the *Alk7* locus of *Alk7*$^{-/-}$ mutant mice allowed us to localize endogenous expression of this gene in pancreatic islets, colocalizing with immunoreactivity for both insulin and glucagon (Fig. S2 *A–C*). By using transgenic mice expressing GFP from a bacterial artificial chromosome (BAC) containing the *Alk7* locus (22), GFP immunoreactivity could be detected in all insulin, glucagon, and somatostatin immunoreactive cells (Fig. S2*D* and data not shown). We conclude that all major cell types in pancreatic islets express the *Alk7* gene at comparable levels in adult pancreas.

Age-Dependent Increase in β-Cell Mass in Pancreas from *Alk7*$^{-/-}$ Mice. Disruption of ALK7 expression had no major effects on islet formation, organization, or generation of all major islet cell types (Fig. S2 and Fig. 3). However, an increase in islet size and β-cell mass was observed in mutant pancreata of 5- and 12-month old animals (Fig. 3 *A* and *B*). β-Cell mass was not significantly affected in 2-month-old mutants. The size of pancreatic β-cells was not different in islets from 12-month-old mutants compared with WT (cell area 101.7 ± 9.41 μm^2 versus 97.9 ± 8.93 μm^2, n =

MEDICAL SCIENCES

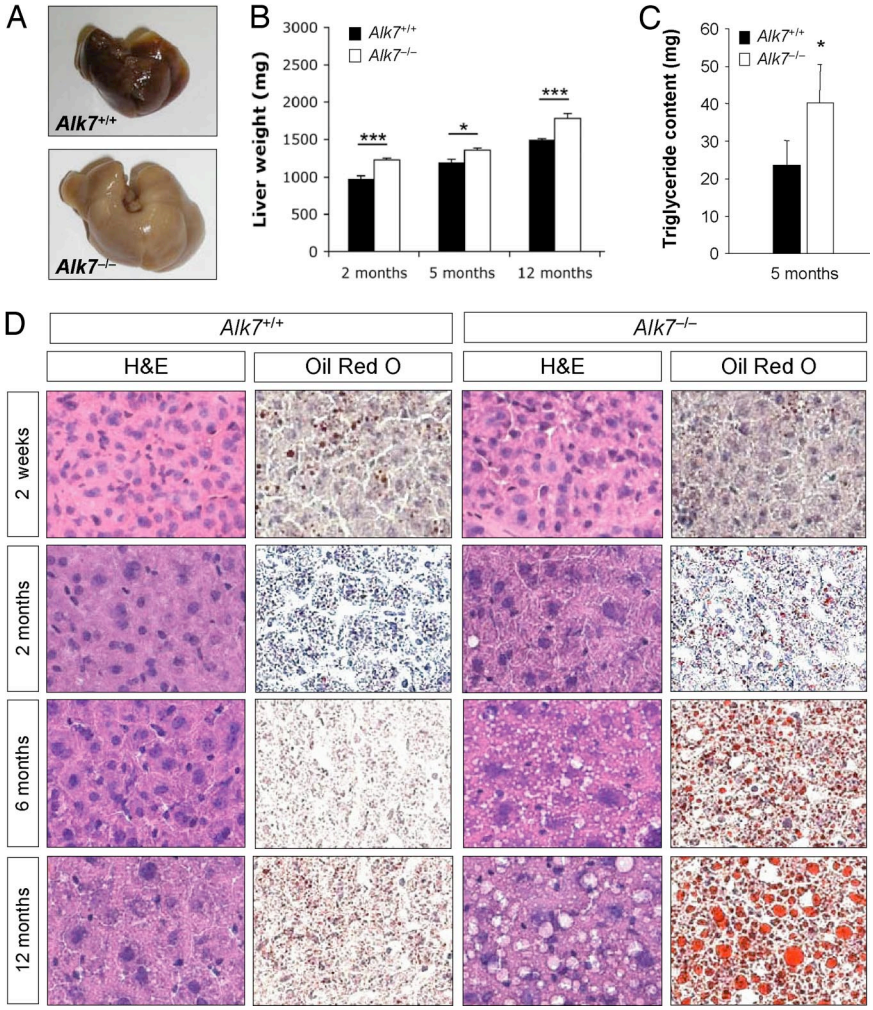

Fig. 2. Age-dependent liver steatosis in *Alk7*$^{-/-}$ mice. (*A*) Macroscopic appearance of livers in 12-month-old WT and *Alk7*$^{-/-}$ mice. (*B*) Wet liver weight in WT and *Alk7*$^{-/-}$ mice at different ages. *, $P \leq 0.05$; ***, $P \leq 0.001$ vs. WT (Student's *t* test). (*C*) Triglyceride content in livers of 5-month-old WT and *Alk7*$^{-/-}$ mice. *, $P \leq 0.05$. (*D*) Histological analysis by H&E and Oil red-O staining of liver sections from WT and *Alk7*$^{-/-}$ mice at different ages. Liver lipid deposits can be seen as red droplets in the Oil red-O images.

18), suggesting that islet enlargement was due to increased cell number. A marked increase in β-cell proliferation was observed in islets from 12-month-old *Alk7*$^{-/-}$ mutants as assessed by Ki67 immunostaining (Fig. 3 *C* and *D*). We could not detect apoptotic cells in either WT or mutant pancreata (data not shown).

Increased Insulin Secretion After Sustained Glucose Stimulation in Islets from *Alk7*$^{-/-}$ Mice. Because the elevated insulin serum levels observed in younger mutants (<5 months of age) could not be satisfactorily explained by changes in β-cell mass, we examined mRNA and protein levels of endocrine hormones in WT and mutant pancreata. However, insulin, glucagon, pancreatic polypeptide, or somatostatin gene expression was not altered in the mutants (Fig. S3 *A* and *B*). Moreover, the relative content of insulin and glucagon protein was not different between mutant and WT pancreata (Fig. S3 *C* and *D*). Because insulin serum levels reflect, to a large extent insulin release, we investigated the ability of islets isolated from 2-month-old mutant and WT pancreata to secrete insulin in response to glucose stimulation. Islets kept at low glucose (3 mM) secreted background levels of insulin regardless of genotype (Fig. 4*A*). Switching from low to high glucose concentration (3–11 mM) induced a marked increase in insulin secretion from both mutant and WT islets (Fig. 4*A*). When WT islets were kept in high glucose (11 mM), lower levels of insulin secretion were observed (Fig. 4*A*), in agreement with β-cell desensitization (23). In contrast, *Alk7*$^{-/-}$ islets maintained in high glucose continued secreting high levels of insulin, resulting in >2-fold higher insulin release than WT (Fig. 4*A*). The sustained response of mutant islets suggests that ALK7 may function as a glucose-dependent negative regulator of insulin secretion.

Alk7 mRNA expression was found to be positively regulated by glucose in pancreatic islets (Fig. 4*B*) in agreement with previous observations (21). Interestingly, islet expression of *Inhibin-βA* and *Inhibin-βB*, respectively encoding activin A and -B, was found to be differentially regulated by glucose, with expression of *Inhibin-βA* decreasing but that of *Inhibin-βB* increasing after glucose stimulation (Fig. 4*B*).

Differential Signaling Activities of Activins A and -B in Pancreatic Islets. Activins A and -B have so far been presumed to elicit similar, if not identical, downstream signaling events. Previous work has indicated that activin A is a positive regulator of β-cell function through stimulation of Ca^{2+} influx, a trigger of insulin secretion (9), but the activities of activin B are unknown. A strong Ca^{2+} influx response was observed after stimulation of WT islets with glucose that could be significantly potentiated by costimulation with activin A (Fig. 5*A*), in agreement with

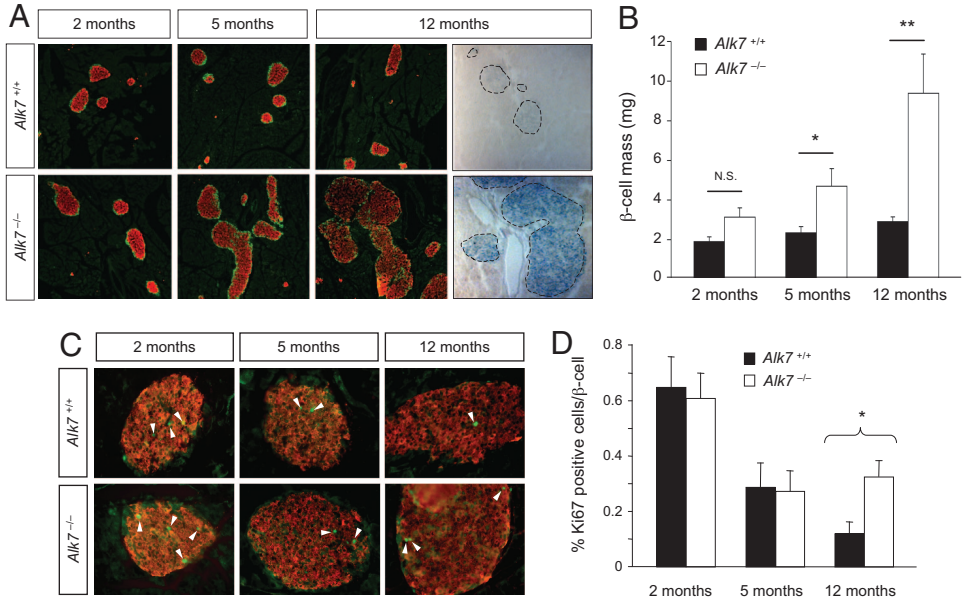

Fig. 3. Age-dependent increase in β-cell mass in pancreas of *Alk7*$^{-/-}$ mice. (*A*) Progressive islet enlargement in pancreas of *Alk7*$^{-/-}$ mice. Shown are double-immunofluorescence micrographs of insulin (red) and glucagon (green) immunoreactivity in sections of WT and *Alk7*$^{-/-}$ mutant islets of the indicated ages. X-gal stainings of sections through 12-month pancreata are shown to the right. (*B*) β-cell mass quantification in pancreatic islets from 2-month-, 5-month-, and 12-month-old WT and mutant animals. Results are expressed as average ± SEM ($n = 6$). N.S., not significantly different; *, $P \leq 0.05$; **, $P \leq 0.01$ (Student's *t* test). (*C*) Analysis of β-cell proliferation in WT and mutant islets. Shown are double-immunofluorescence micrographs of insulin (red) and Ki67 (green) immunoreactivity in sections of WT and mutant islets of the indicated ages. Ki67^{+} nuclei are indicated with arrowheads. (*D*) Quantitative analysis of β-cell proliferation in pancreatic islets from 2-month-, 5-month-, and 12-month-old WT and mutant animals. Results are expressed as average ± SEM (75 islets from 5 different animals per genotype). *, $P = 0.015$ (Student's *t* test).

previous observations. In contrast, administration of activin B depressed glucose-stimulated Ca^{2+} influx compared with glucose alone (Fig. 5*A*). In the absence of glucose, activin B had no effect on Ca^{2+} influx in WT cells but induced a significant response in mutant cells (Fig. 5*B*), in agreement with a negative role for ALK7 in Ca^{2+} signaling by activin B. In contrast, activin B stimulated Smad2 phosphorylation in both WT and mutant islets at comparable levels (Fig. 5*C*), suggesting that ALK7 is not required for the activation of this pathway in response to activin B in islet cells. Together, these results show that activins A and -B have opposite effects on Ca^{2+} influx in islet cells and support a role for ALK7 as a negative regulator of insulin release through modulation of activin B signaling in β-cells.

Hyperinsulinemia in Mice Lacking Activin B. An important prediction of the above findings is that lack of activin B should, similarly to lack of ALK7, also result in hyperinsulinemia. At 2 months of age, *InhβB*$^{-/-}$ mice displayed 2-fold higher insulin serum levels compared with WT controls and were, in this respect, indistinguishable from age-matched *Alk7*$^{-/-}$ mice (Fig. 5*D*). The effects of the *Alk7*$^{-/-}$ and *InhβB*$^{-/-}$ mutations were not additive, because double-mutant mice displayed insulin serum levels that were comparable with those observed in the single mutants (Fig. 5*D*). This is in agreement with the notion that activin B and ALK7 function in a common pathway to regulate insulin secretion.

Discussion

In the present study, we have investigated the role of the TGF-β superfamily receptor ALK7 in the organization and function of the endocrine pancreas. Our studies indicate that mice lacking ALK7 develop an age-dependent syndrome involving hyperinsulinemia, reduced insulin sensitivity, liver steatosis, impaired

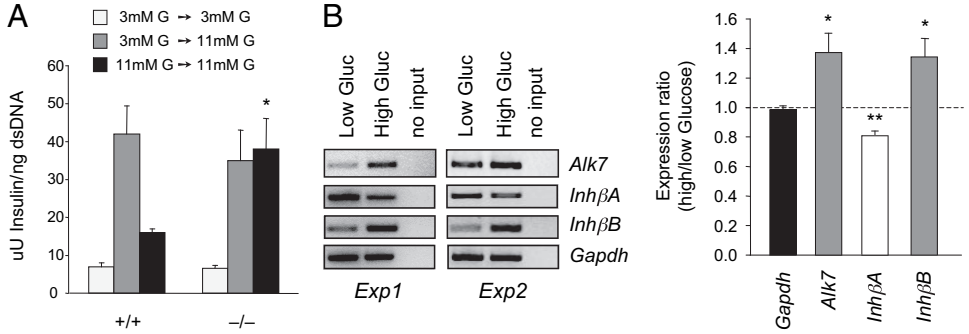

Fig. 4. Increased glucose-stimulated insulin secretion in islets from *Alk7*$^{-/-}$ mice and differential regulation of activin expression by glucose. (*A*) Glucose-stimulated insulin secretion in isolated islets from 2-month-old *Alk7*$^{-/-}$ mutant and WT mice. Results are expressed as average ± SEM ($n = 4$–6). G, glucose. *, $P \leq 0.05$ vs. +/+ (Student's *t* test). (*B*) RT-PCR analysis of gene expression in pancreatic islets of 2-month-old WT mice after overnight incubation in low (3 mM) or high (11 mM) glucose concentration. PCR results from two independent experiments are shown. The histogram shows quantitative analysis of five independent RT-PCR experiments expressed as averages of relative expression ratios (high vs. low glucose) ± SEM. *, $P \leq 0.05$; **, $P \leq 0.01$.

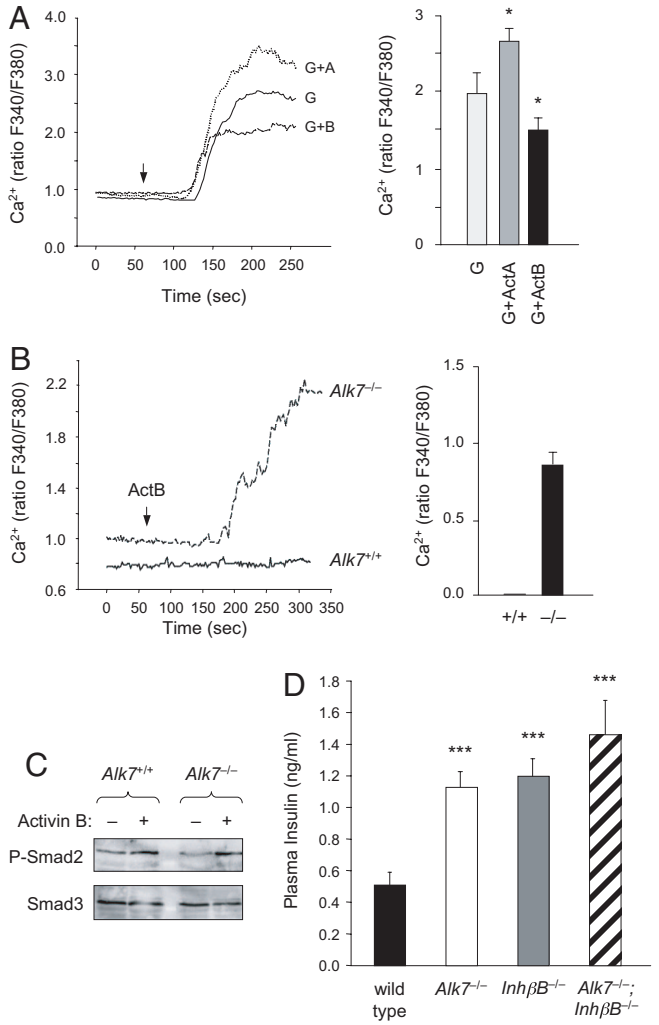

Fig. 5. Differential β-cell Ca^{2+} responses to activins A and B and hyperinsulinemia in $Inh\beta B^{-/-}$ mice. (*A*) Cytoplasmic free-Ca^{2+} concentration in dissociated WT islet cells after stimulation with 11 mM glucose (G), alone or in combination with activin A (ActA; 5 nM) or activin B (ActB; 10 nM). The arrow indicates time of stimulation. Histogram plots integrated Ca^{2+} responses for the indicated conditions. Results are expressed as average ± SEM ($n = 3$). *, $P \leq 0.05$ vs. G (Student's *t* test). (*B*) Ca^{2+} responses in WT and $Alk7^{-/-}$ dissociated islet cells after stimulation with activin B (ActB; 10 nM) together with 3 mM glucose (arrow). Histogram plots integrated Ca^{2+} responses for the indicated conditions. Results are expressed as average ± SEM ($n = 3$). (*C*) Phospho-Smad2 immunoblots of lysates from islets of WT and $Alk7^{-/-}$ mice after 15-min incubation with activin B. Control reprobing with anti-Smad3 antibodies is shown below. (*D*) Insulin serum levels after 5-h fasting in WT, $Alk7^{-/-}$, $Inh\beta B^{-/-}$, and $Alk7^{-/-}$;$Inh\beta B^{-/-}$ mice. Results are expressed as average ± SEM. ***, $P \leq 0.001$ vs. WT (Student's *t* test).

glucose tolerance, and islet enlargement, suggesting that this receptor plays an important role in the control of metabolic homeostasis.

Our morphological and histological studies did not support a major developmental role for ALK7 in pancreas organogenesis or generation of the major cell types in pancreatic islets. On the other hand, we found that lack of ALK7 produces an imbalance in the circuits that control glucose-stimulated insulin release in β-cells. Our analysis of Ca^{2+} responses in WT and mutant islets revealed unexpectedly opposite actions of activins A and -B in the regulation of glucose-dependent Ca^{2+} influx into the β-cell and a negative role for activin B on Ca^{2+} influx meditated by ALK7. The fact that glucose decreased islet expression of activin A (a positive regulator of Ca^{2+} influx), whereas it increased that of activin B (a negative regulator of Ca^{2+} influx) and of its receptor ALK7 uncovered a previously unknown negative-feedback loop mediated by autocrine activin signaling that regulates glucose-dependent Ca^{2+} influx in islet cells. We propose that the absence of ALK7 renders this feedback loop defective, leading to increased insulin secretion under sustained glucose stimulation. In agreement with this notion, mice lacking activin B showed elevated insulin serum levels comparable with those observed in $Alk7^{-/-}$ mutants. If ALK7 and activin B affected insulin serum levels via different pathways, their simultaneous elimination would be expected to result in additive effects. However, double and single mutants displayed comparable insulinemia in agreement with the notion that activin B acts via ALK7 to negatively regulate insulin serum levels.

Although lack of activin B phenocopied the hyperinsulinemia observed in mice lacking ALK7, $Inh\beta B^{-/-}$ mutants do not develop insulin resistance, liver steatosis, or islet enlargement (P.B. and C.I., unpublished observations). This indicates that those phenotypes may be the consequence of deficits in the activities of other ALK7 ligands. We have recently found that GDF-3 signals through ALK7 and regulates accumulation of adipose tissue and diet-induced obesity (14). Although neither $Inh\beta B^{-/-}$ or $Gdf3^{-/-}$mutants show signs of reduced insulin sensitivity or liver steatosis (this study and ref. 14), those phenotypes could be the result of defects in the activities of yet additional ALK7 ligands or, perhaps more interestingly, arise as a synergistic effect of combined hyperinsulinemia and reduced fat deposition caused by abnormalities in both activin B and GDF3 signaling. Although liver steatosis is a well known contributor to insulin resistance, the lack of ALK7 expression in this organ indicates that this phenotype must be a secondary defect in the mutants. Moreover, the delayed onset of β-cell mass increase in $Alk7^{-/-}$ mutants suggests that this is most likely an indirect consequence of decreased insulin sensitivity, as it has been observed in other systems (24). On the other hand, the fact that hyperinsulinemia developed independently of insulin resistance in mice lacking activin B supports the idea of its being a primary defect in the mutants, a notion that is reinforced by the appearance of elevated insulin serum levels before any detectable decline in insulin sensitivity in $Alk7^{-/-}$ mice. Together, our findings are most consistent with the idea that hyperinsulinemia originates as an early cell-autonomous defect in the regulation of glucose-stimulated insulin secretion in mutant β-cells.

The differential regulation of glucose-dependent Ca^{2+} influx in islet cells by activin A and -B represents an example of antagonistic signaling activities among these activins that has not been previously noted. Because both ligands are able to activate the ALK4 receptor, we have hypothesized that their differential effects on Ca^{2+} signaling may be mediated by ALK7, through which only activin B can signal. In agreement with this, activin B showed no effect on Ca^{2+} influx in WT cells in the absence of glucose but elicited a marked response in cells lacking ALK7, presumably via the remaining ALK4 receptor. Whether ALK7 antagonizes ALK4 directly or mediates a downstream signaling event that opposes some of the activities of that receptor is unclear at present. In contrast to its differential effects on Ca^{2+} signaling, activin B was able to stimulate Smad2 phosphorylation in both WT and mutant islets with equal potency, suggesting that Ca^{2+} responses may be elicited by Smad-independent pathways. Interestingly, the short time course during which activins are able to modulate Ca^{2+} influx in islet cells (i.e., ≈2 min) is also in agreement with a nontranscriptional signaling event. A recent report has indicated that activin B is more potent than activin A at inducing expression of the pancreatic marker Pdx1 in differentiating human embryonic stem cells (25).

In conclusion, our results indicate that ALK7 plays important and previously unrecognized roles in the control of metabolic homeostasis. Within pancreatic islets, our findings uncovered an unexpected antagonism between activins A and -B in the control

of β-cell function through their differential ability to regulate Ca^{2+} signaling and revealed the activin B receptor ALK7 as a negative regulator of insulin secretion in β-cells.

Materials and Methods

Animals. The generation of the *Alk7* null allele has been described (17). All experiments in the present study were performed on mice back-bred (for 10 generations) to a C57BL/6 background. *Inhβ*$B^{-/-}$ mice (26) were obtained as frozen embryos from The Jackson Laboratories (stock number 002442). Animal protocols were approved by Stockholms Norra Djurförsöksetiska Nämnd and were in accordance with ethical guidelines of the Karolinska Institute (*SI Text*).

Immunohistochemistry, X-Gal Staining, and Liver Histological Analyses. Adult pancreata were harvested in phosphate buffer (pH 7.4), fixed overnight in cold 4% paraformaldehyde (PFA), and cryoprotected in 30% sucrose before freezing in OCT compound (Tissues Tek). H&E and Oil red-O (Sigma) staining were performed on frozen liver sections according to standard protocols. (*SI Text*).

Islet Morphometry and Proliferation Assays. Quantification of β-cell mass was done by the planimetry method (27), and analysis of β-cell proliferation was performed as described (28) (*SI Text*).

Metabolic Measurements, Insulin, and Glucose Tolerance Tests. Blood glucose was measured by tail-tip bleeding by using a FreeStyle mini Glucometer (Abbott). Serum insulin measurements were done by RIA using rat insulin (Novo Nordisk) standard (*SI Text*).

Islet Insulin Release and Cytoplasmic Free Ca^{2+}. Pancreatic islets were isolated from mice by collagenase dispersion and, when required, mechanically disrupted into cells with Cell Dissociation Buffer (GIBCO). For studies of glucose-induced insulin-secretion measurements of cytoplasmic free Ca^{2+}, see *SI Text*.

RT-PCR Analysis and Western Blot Analysis. Total RNA extraction was done on isolated islets by using a RNeasy Mini kit (Qiagen) according to the manufacturer's instructions. For Western blot analysis, antibodies against phospho-Smad2 (Cell Signaling Technology), and Smad3 (Zymed) were used (*SI Text*).

Statistical Analysis. Each variable was analyzed by using the unpaired Student's *t* test unless indicated. For all analyses, a *P* value of <0.05 was considered significant. Results are given as means ± SEM. All analyses were performed by using Prism4 Software (GraphPad).

ACKNOWLEDGMENTS. We thank Barbara Cannon, Jan Nedergaard, Henrik Jörnvall, and Juleen Zierath for valuable discussions; and Bihu Gao, Mehrnaz Mehrkash, Dagmar Galter, Maj Sundblom, Eva Björkstrand, Annika Olson, and Ernst Brodin for help with initial experiments. This work was supported by the Swedish Foundation for Strategic Research, Swedish Cancer Society, Swedish Research Council (C.F.I.), the Family Erling–Persson Foundation, Swedish Diabetes Association, the Novo-Nordisk Foundation, and the Beth von Kantzows Foundation (P.-O.B.). P.B. was supported by a fellowship from the Wenner Gren Foundations and E.R. was supported by a Marie Curie Fellowship.

1. Shi Y, Massague J (2003) Mechanisms of TGF-beta signaling from cell membrane to the nucleus. *Cell* 113:685–700.
2. ten Dijke P, Hill CS (2004) New insights into TGF-beta-Smad signalling. *Trends Biochem Sci* 29:265–273.
3. Moustakas A, Heldin CH (2005) Non-Smad TGF-beta signals. *J Cell Sci* 118:3573–3584.
4. Kim SK, Hebrok M (2001) Intercellular signals regulating pancreas development and function. *Genes Dev* 15:111–127.
5. Shi Y, *et al.* (2005) Inducing embryonic stem cells to differentiate into pancreatic beta cells by a novel three-step approach with activin A and all-*trans* retinoic acid. *Stem Cells* 23:656–662.
6. Ide M, Shintani Y, Kosaka M, Sano T, Saito S (1996) Localization of activin A/EDF in the normal and diabetic rat pancreas: Immunohistochemical and *in Situ* hybridization studies. *Endocr Pathol* 7:229–236.
7. Maldonado TS, *et al.* (2000) Ontogeny of activin B and follistatin in developing embryonic mouse pancreas: implications for lineage selection. *J Gastrointest Surg* 4:269–275.
8. Totsuka Y, Tabuchi M, Kojima I, Shibai H, Ogata E (1988) A novel action of activin A: stimulation of insulin secretion in rat pancreatic islets. *Biochem Biophys Res Commun* 156:335–339.
9. Shibata H, *et al.* (1993) Activin A increases intracellular free calcium concentrations in rat pancreatic islets. *FEBS Lett* 329:194–198.
10. Mukherjee A, *et al.* (2007) FSTL3 deletion reveals roles for TGF-β family ligands in glucose and fat homeostasis in adults. *Proc Natl Acad Sci USA* 104:1348–1353.
11. Smart NG, *et al.* (2006) Conditional expression of Smad7 in pancreatic beta cells disrupts TGF-beta signaling and induces reversible diabetes mellitus. *PLoS Biol* 4:e39.
12. Reissmann E, *et al.* (2001) The orphan receptor ALK7 and the activin receptor ALK4 mediate signaling by Nodal proteins during vertebrate development. *Genes Dev* 15:2010–2022.
13. Andersson O, Reissmann E, Jörnvall H, Ibáñez CF (2006) Synergistic interaction between Gdf1 and Nodal during anterior axis development. *Dev Biol* 293:370–381.
14. Andersson O, Korach-Andre M, Reissmann E, Ibáñez CF, Bertolino P (2008) Growth/differentiation factor 3 signals through ALK7 and regulates accumulation of adipose tissue and diet-induced obesity. *Proc Natl Acad Sci USA* 105:7252–7256.
15. Tsuchida K, *et al.* (2004) activin isoforms signal through type I receptor serine/threonine kinase ALK7. *Mol Cell Endocrinol* 220:59–65.
16. Rydén M, *et al.* (1996) A novel type I receptor serine-threonine kinase predominantly expressed in the adult central nervous system. *J Biol Chem* 271:30603–30609.
17. Jörnvall H, Reissmann E, Andersson O, Mehrkash M, Ibáñez CF (2004) ALK7, a receptor for nodal, is dispensable for embryogenesis and left–right patterning in the mouse. *Mol Cell Biol* 24:9383–9389.
18. Bondestam J, *et al.* (2001) cDNA cloning, expression studies and chromosome mapping of human type I serine/threonine kinase receptor ALK7 (ACVR1C). *Cytogenet Cell Genet* 95:157–162.
19. Lorentzon M, Hoffer B, Ebendal T, Olson L, Tomac A (1996) Habrec1, a novel serine/threonine kinase TGF-beta type I-like receptor, has a specific cellular expression suggesting function in the developing organism and adult brain. *Exp Neurol* 142:351–360.
20. Watanabe R, *et al.* (1999) The MH1 domains of smad2 and smad3 are involved in the regulation of the ALK7 signals. *Biochem Biophys Res Commun* 254:707–712.
21. Zhang N, *et al.* (2006) activin receptor-like kinase 7 induces apoptosis of pancreatic beta cells and beta cell lines. *Diabetologia* 49:506–518.
22. Gong S, *et al.* (2003) A gene expression atlas of the central nervous system based on bacterial artificial chromosomes. *Nature* 425:917–925.
23. Grodsky GM, Bolaffi JL (1992) Desensitization of the insulin-secreting beta cell. *J Cell Biochem* 48:3–11.
24. Bouwens L, Rooman I (2005) Regulation of pancreatic beta-cell mass. *Physiol Rev* 85:1255–1270.
25. Frandsen U, Porneki AD, Floridon C, Abdallah BM, Kassem M (2007) Activin B mediated induction of Pdx1 in human embryonic stem cell derived embryoid bodies. *Biochem Biophys Res Commun* 362:568–574.
26. Vassalli A, Matzuk MM, Gardner HA, Lee KF, Jaenisch R (1994) Activin/inhibin beta B subunit gene disruption leads to defects in eyelid development and female reproduction. *Genes Dev* 8:414–427.
27. Bonner-Weir S (2001) Beta-cell turnover: Its assessment and implications. *Diabetes 50* Suppl 1:S20–S4.
28. Krishnamurthy J, *et al.* (2006) p16INK4a induces an age-dependent decline in islet regenerative potential. *Nature* 443:453–457.

Supporting Information

Bertolino *et al.* 10.1073/pnas.0801285105

SI Text

Discussion

Unlike ALK7, the majority of TGF-β superfamily receptors investigated so far have shown positive effects on pancreatic islet growth and function. Kim *et al.* (1) reported that inactivating mutations in genes encoding type II activin receptors ActRIIA and B negatively affected the development of pancreatic islets, resulting in islet hypoplasia, hypoinsulinemia, and impaired glucose tolerance (1). However, it has remained unclear to what extent those postnatal phenotypes were the result of developmental defects in foregut patterning and islet differentiation or of postembryonic roles of activin signaling in pancreatic islet function. Moreover, manipulation of activin type II receptors, which can mediate the actions of both activin A and -B, does not resolve possibly distinct contributions of the two activins to β-cell function. The fact that adult overexpression of Smad7, a cytoplasmic inhibitor of Smad signaling downstream of activin and TGF-β receptors, resulted in hypoinsulinemia (2) suggests that the positive effects of activins on pancreatic islets are likely mediated by Smad-dependent gene transcription. However, this leaves open the possibility that, through Smad-independent pathways, activins and TGF-βs may exert other effects on β-cell function. A recent report has indicated that mice lacking the activin inhibitor follistatin-like 3 (FSTL3) develop enlarged pancreatic islets and a moderate increase in insulin serum levels by 9 months of age (3), consistent with a positive role for activins in islet development and function. Interestingly, however, FSTL3 has 10-fold higher affinity for activin A than for activin B (4), suggesting that the consequences of its inactivation may predominantly be due to augmented activin A signaling. Because of its ability to signal through both ALK4 and ALK7, activin B is likely to afford a different repertoire of activities compared with activin A, a notion that is reinforced by our observations indicating that activin B, in contrast to activin A, primarily acts as a negative regulator of insulin release *in vivo*.

Materials and Methods

Animals. A7-GFP$^+$ mice were obtained as frozen embryos from the Gensat collection (stock Tg(Acvr1c-EGFP)1-Gsat/Mmmh) (5). Embryo transfer was performed at the Karolinska Institute transgenic animal core facility and all animals were housed under standard conditions in a pathogen-free environment with food and water ad libitum.

Immunohistochemistry, X-Gal Staining, and Liver Histological Analyses. Immunostaining was performed on 8- to 12-μm-thick serial cryosections by following standard procedures. Primary antibodies against GFP (1/1,000; Abcam), insulin (1/1,000; DAKO), glucagon (1/500; DAKO and 1/500; LincoResearch) and Ki67 (1/50; Abcam) were used in combination with FITC- and TRITC-conjugated secondary antibodies (1/200; Jackson ImmunoResearch) as appropriate. Fluorescence images were captured and analyzed on a Zeiss Axioskop2 microscope coupled with a Jenoptik Jena camera and OpenLab Software (Improvision). X-gal staining was performed on tissue whole mounts or cryosections postfixed in glutaraldehyde according to standard procedures. Combined X-gal staining and immunofluorescence were done as described (6). Immunofluorescence for insulin and glucagon were done before overnight incubation in X-gal substrate. Sections were analyzed as described above, and images were processed and merged by using OpenLab software.

Islet Morphometry and Proliferation Assays. Briefly, pancreata were cleared of fat and lymph nodes and weighted before fixation. Cryosections (12 μm) were stained for insulin and glucagon, and a section covering the entire pancreas was randomly selected from each animal and photographed. Single images were assembled together to reconstruct an entire pancreas image. Exocrine and insulin-positive areas were quantified with OpenLab software to obtain the proportion of β-cells in each pancreas section. Total β-cell mass was then calculated by multiplying this amount by the total weight of the corresponding pancreas. Each quantification was performed blind to the genotype of the animal.

For islet proliferation analysis, 12-μm-thick pancreas sections were immunostained for Ki67 and insulin and counterstained with DAPI (Vector Laboratories). At least 75 randomly chosen islets from five independent age-matched pancreata were analyzed per genotype. The number of Ki67-positive cells per unit of β-cell area was determined by using OpenLab software. On the same sections, β-cell density was determined as the number of DAPI-positive nuclei per unit of β-cell area. The percentage of Ki67-positive cells among the β-cell population was calculated as the ratio between Ki67 and β-cell densities $\times$ 100.

Metabolic Measurements, Insulin, and Glucose Tolerance Tests. Serum glucagon measurements were done in animals fasted overnight by RIA using human glucagon (Eurodiagnostica) standards. Insulin and glucagon total content were assessed by RIA on acid–ethanol extracts of whole pancreas and normalized to total protein concentration. Islets insulin total contents were determined by RIA using pooled isolated islets and extracted for protein and DNA with M-PER (Pierce). PicoGreen double-stranded DNA (dsDNA) quantification kit (Molecular Probes) was used to quantify dsDNA, used for normalization. Glucose tolerance tests were performed after 5 h (2-month-old animals) or overnight (5-month-old animals) fasting, whereas insulin tolerance tests were done with mice that were starved for 3 h. Animals were injected (i.p.) with either 1.5 g/kg of body weight of dextrose (Sigma) or 1 unit/kg of body weight of recombinant human insulin (Actrapid; Novo Nordisk). Glucose levels were measured from blood collected from the tail immediately before and 15, 30, 60, 90, and 120 min after the injection. Triglycerides were analyzed with an enzymatic calorimetric method (Triglyceride/GB; Roche) after elimination of free glycerol.

Islet Insulin Release and Cytoplasmic Free Ca^{2+}. For studies of glucose-induced insulin secretion, isolated islets were first cultured overnight at 37°C (5% CO_2) in RPMI medium 1640 containing 11.1 mM glucose and supplemented with 100 μg/ml streptomycin, 100 μg/ml penicillin, 2 mM glutamine, and 10% FBS. Ten islets were pooled in batches and incubated at 37°C for 45 min in a Hepes buffer (pH 7.4) containing 125 mM NaCl, 5.9 mM KCl, 1.2 mM $MgCl_2$, 1.28 mM $CaCl_2$, and 3 mM glucose (or 11 mM glucose when indicated). BSA was added at a concentration of 1 mg/ml. This was followed by incubation in the same buffer containing either 3 or 11 mM glucose for 60 min at 37°C. At the end of the incubation, the buffer was assayed for secreted insulin by RIA, and the islets were collected for DNA normalization of insulin levels as described above. For measurements of cytoplasmic free Ca^{2+} concentration, islets were attached to coverslips and incubated overnight in 37°C (5% CO_2) in RPMI medium 1640. The cells were loaded with 2 mM fura-2/

acetoxymethylester (Molecular Probes) at 37°C for 30 min. Changes in $[Ca^{2+}]_I$ were measured by using a Spex fluorolog-2 CM1T11I system connected to an inverted microscope (Axiovert 35M; Zeiss). The emission of the two excitation wavelengths of 340 and 380 nm were used to calculate the fluorescent ratio (F340/F380), reflecting changes in $[Ca^{2+}]_I$.

RT-PCR Analysis and Western Blotting. PCRs were performed on 1 μg of reverse-transcribed cDNA (SuperScript II RT kit; Invitrogen) using primers for *Alk7*, *Inhibin-βA*, *Inhibin-βB*, *Gapdh*, *Insulin*, *Glucagon*, *Somatostatin*, and *Pancreatic polypeptide* as described (7–9). After gel electrophoresis, RT-PCR bands were quantified with QuantityOne (Biolabs).

1. Kim SK, *et al.* (2000) Activin receptor patterning of foregut organogenesis. *Genes Dev* 14:1866–1871.
2. Smart NG, *et al.* (2006) Conditional expression of Smad7 in pancreatic beta cells disrupts TGF-beta signaling and induces reversible diabetes mellitus. *PLoS Biol* 4:e39.
3. Mukherjee A, *et al.* (2007) FSTL3 deletion reveals roles for TGF-β family ligands in glucose and fat homeostasis in adults. *Proc Natl Acad Sci USA* 104:1348–1353.
4. Schneyer A, Schoen A, Quigg A, Sidis Y (2003) Differential binding and neutralization of activins A and B by follistatin and follistatin like-3 (FSTL-3/FSRP/FLRG). *Endocrinology* 144:1671–1674.
5. Gong S, *et al.* (2003) A gene expression atlas of the central nervous system based on bacterial artificial chromosomes. *Nature* 425:917–925.
6. Kockel L, *et al.* (2006) An amylase/Cre transgene marks the whole endoderm but the primordia of liver and ventral pancreas. *Genesis* 44:287–296.
7. Gittes GK, Rutter WJ (1992) Onset of cell-specific gene expression in the developing mouse pancreas. *Proc Natl Acad Sci USA* 89:1128–1132.
8. Jörnvall H, Reissmann E, Andersson O, Mehrkash M, Ibáñez CF (2004) ALK7, a receptor for nodal, is dispensable for embryogenesis and left-right patterning in the mouse. *Mol Cell Biol* 24:9383–9389.
9. Watabe T, *et al.* (2003) TGF-beta receptor kinase inhibitor enhances growth and integrity of embryonic stem cell-derived endothelial cells. *J Cell Biol* 163:1303–1311.

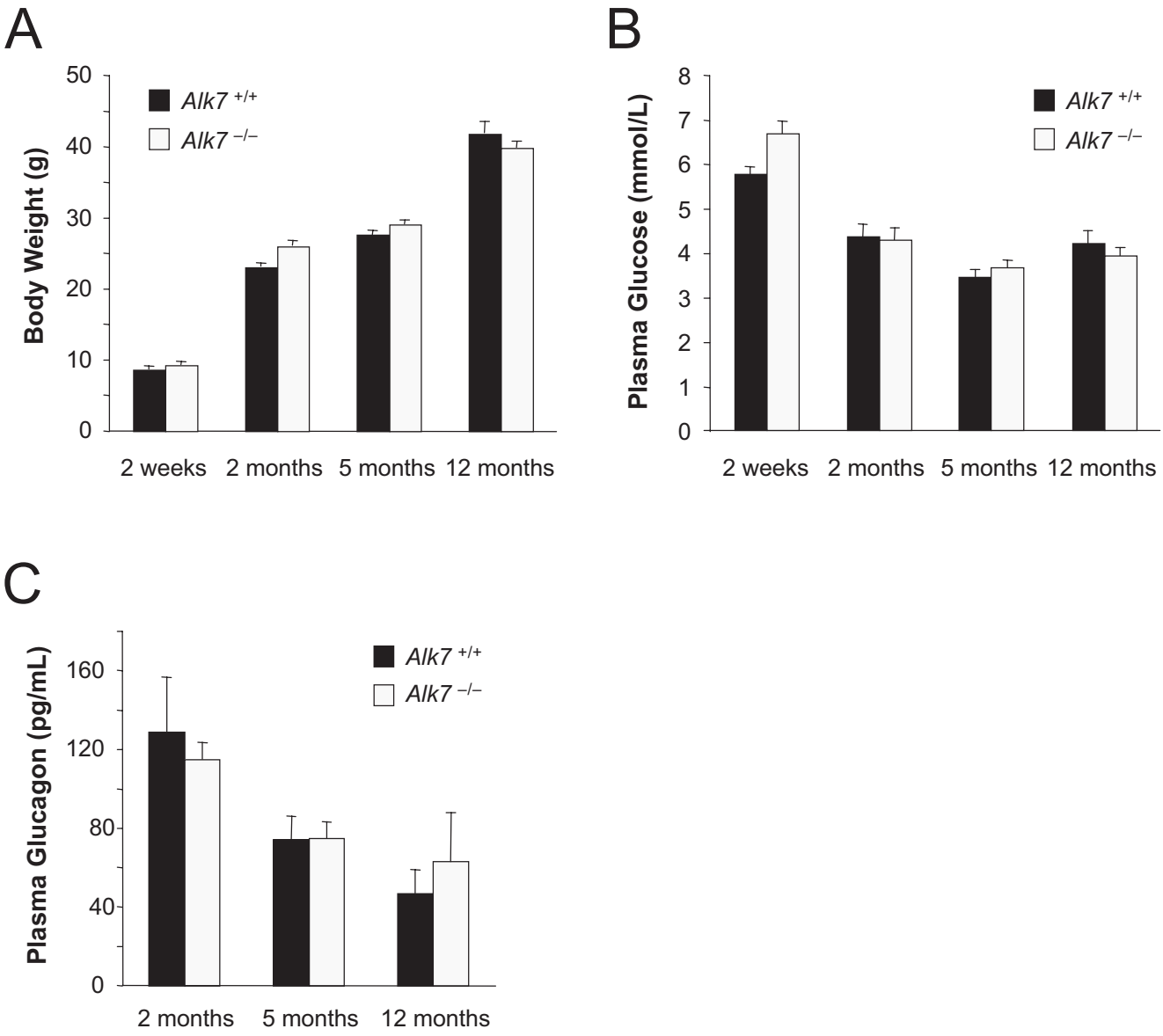

Fig. S1. Body weight and glucose and glucagon serum levels in WT and *Alk7*$^{-/-}$ mice. (*A*) Body weight of chow-fed WT (n = 9–15) and *Alk7*$^{-/-}$ (n = 11–17) mice. (*B*) Glycemia after overnight fasting in wild type (n = 5–20) and *Alk7*$^{-/-}$ (n = 6–20) mice. (*C*) Glucagon serum levels after overnight fasting in WT (n = 3–6) and *Alk7*$^{-/-}$ (n = 3–5) mice.

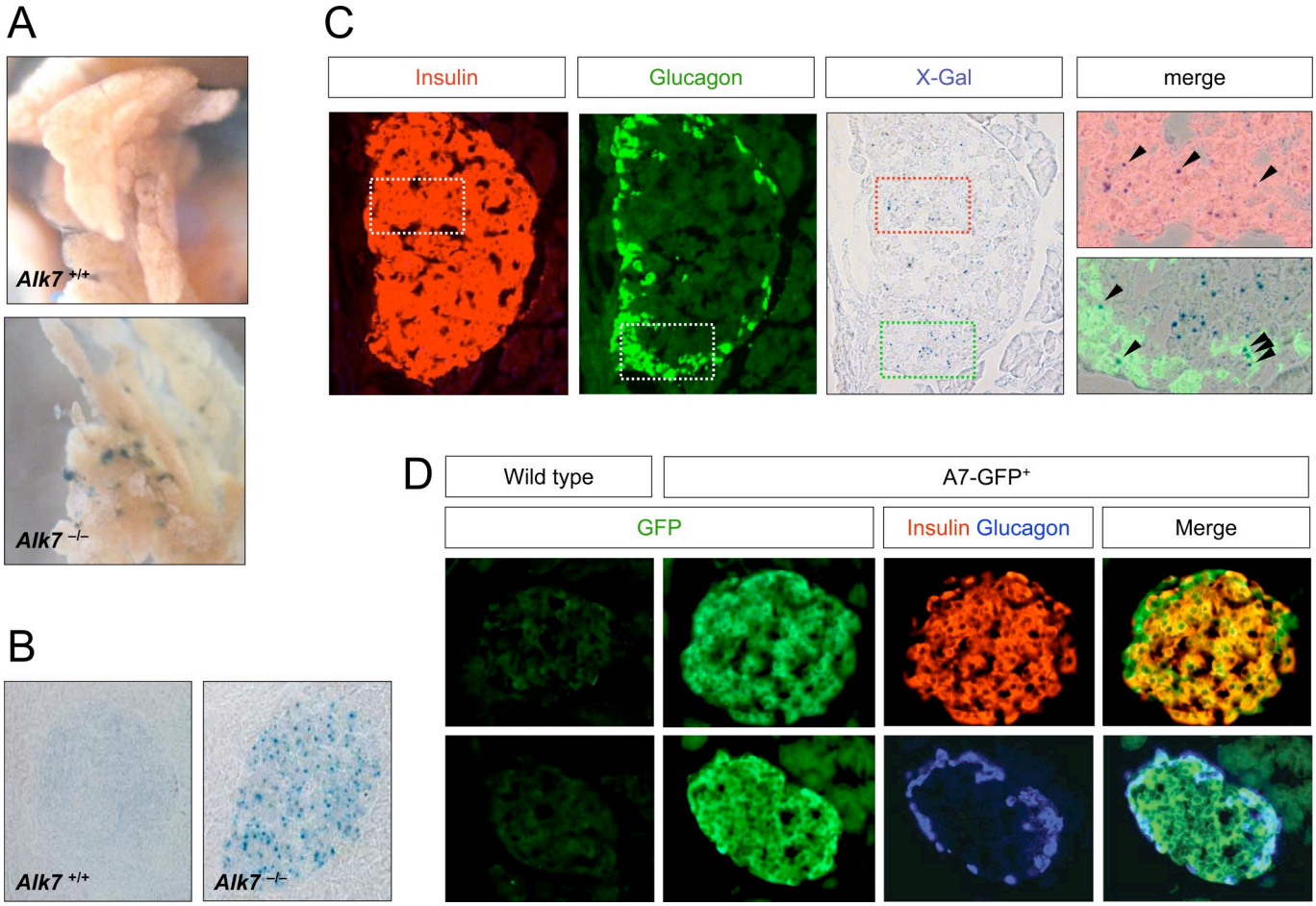

Fig. S2. Alk7 expression in mouse endocrine pancreas. (*A*) Whole-mount X-gal stainings of pancreata from newborn WT (*Alk7*$^{+/+}$) and mutant (*Alk7*$^{-/-}$) mice. (*B*) X-gal stainings of sections through pancreatic islets from 3-month-old WT and *Alk7* mutant mice. (*C*) Colocalization of X-gal precipitates with insulin and glucagon immunoreactivity in sections of pancreatic islets from 3-month-old *Alk7*$^{-/-}$ mice. Areas boxed in insulin, glucagon, and X-gal images are shown as high magnification, merged images to the right. (*D*) Colocalization of GFP expression with insulin and glucagon in islets of A7-GFP^{+} mice. No GFP immunoreactivity could be detected in islets from WT animals.

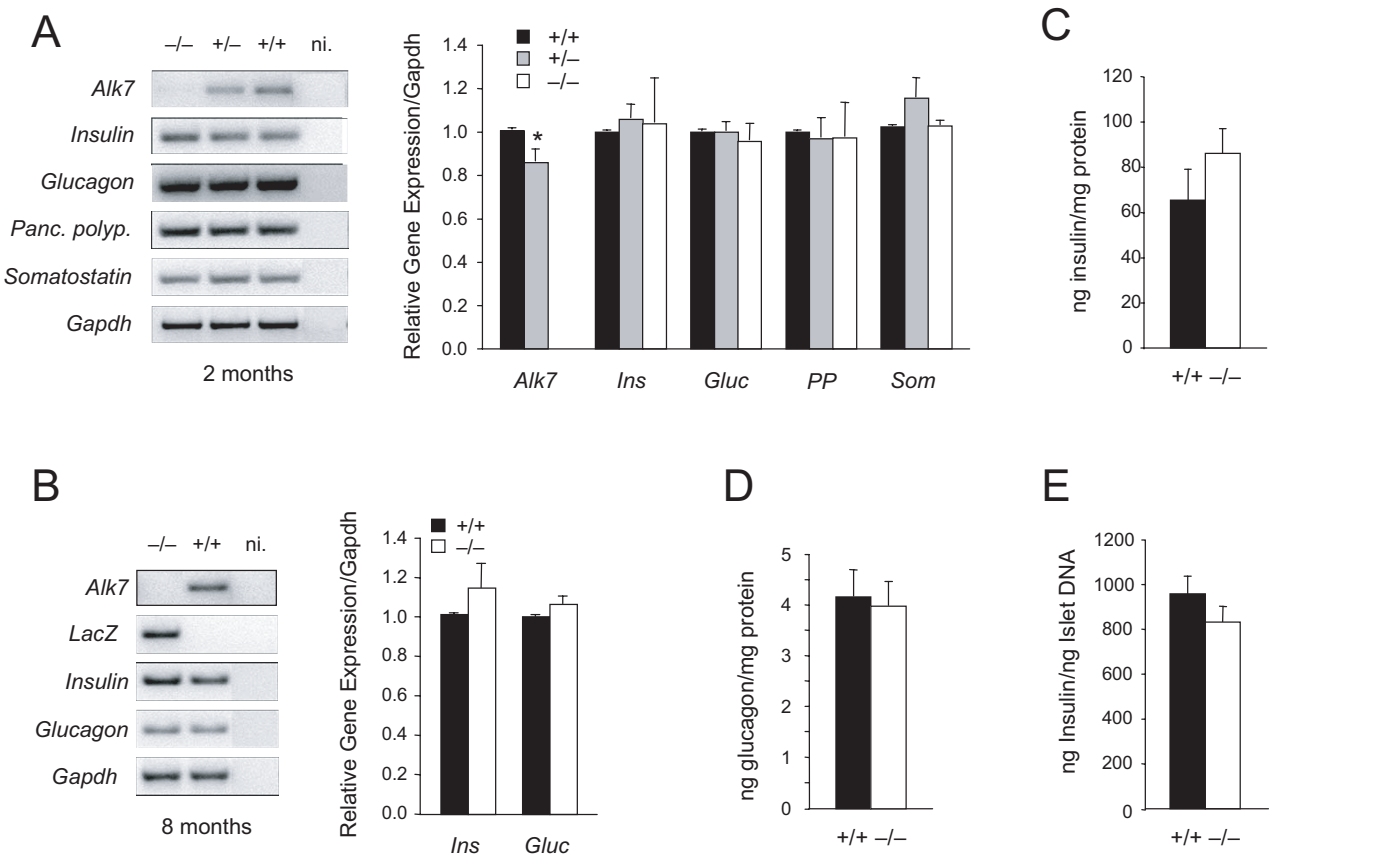

Fig. S3. Insulin and glucagon expression in 2-month- and 8-month-old WT and *Alk7*$^{-/-}$ mutant pancreas. (*A*) RT-PCR analysis of gene expression in pancreatic islets of 2-month-old WT and *Alk7*$^{-/-}$ mice. ni., no input. *, $P \leq 0.05$; $n = 3$ independent experiments. (*B*) RT-PCR analysis of gene expression in pancreatic islets of 8-month-old WT and *Alk7*$^{-/-}$ mice. n.i., no input. $n = 3$ independent experiments. (*C*) Pancreatic insulin content normalized to total protein in 2-month-old WT and *Alk7*$^{-/-}$ mice. $n = 6$. (*D*) Pancreatic glucagon content normalized to total protein in 2-month-old WT and *Alk7*$^{-/-}$ mice. $n = 6$. (*E*) Islet insulin content normalized to total DNA in 2-month-old WT and *Alk7*$^{-/-}$ mice. $n = 6$.